Talanta 82 (2010) 177–183

Contents lists available at ScienceDirect

Talanta

journal homepage: www.elsevier.com/locate/talanta

Preparation of gold nanoparticles on eggshell membrane and their biosensing application

Baozhan Zheng[a,1], Lei Qian[b], Hongyan Yuan[a], Dan Xiao[a,b,*], Xiupei Yang[c,2], Man Chin Paau[d], Martin M.F. Choi[d,**]

[a] College of Chemical Engineering, Sichuan University, Chengdu 610064, PR China
[b] College of Chemistry, Sichuan University, Chengdu 610064, PR China
[c] College of Chemistry and Chemical Engineering, China West Normal University, Nanchong 637002, PR China
[d] Department of Chemistry, Hong Kong Baptist University, 224 Waterloo Road, Kowloon Tong, Hong Kong, China

ARTICLE INFO

Article history:
Received 13 January 2010
Received in revised form 7 April 2010
Accepted 8 April 2010
Available online 14 April 2010

Keywords:
Gold nanoparticles
Eggshell membrane
Biocatalysis
Glucose biosensors

ABSTRACT

A facile green biosynthesis method has been successfully developed to prepare gold nanoparticles (AuNPs) of various core sizes (25 ± 7 nm) using a natural biomaterial, eggshell membrane (ESM) at ambient conditions. In situ synthesis of AuNPs-immobilized ESM is conducted in a simple manner by immersing ESM in a pH 6.0 aqueous solution of $HAuCl_4$ without adding any reductant. The formation of AuNPs on ESM protein fibers is attributed to the reduction of Au(III) ions to Au(0) by the aldehyde moieties of the natural ESM fibers. Energy dispersive X-ray spectroscopy, scanning electron microscopy, X-ray photoelectron spectroscopy, and X-ray powder diffraction unambiguously identify the presence of AuNPs on ESM. The effect of pH on the in situ synthesis of AuNPs on ESM has been investigated in detail. The pH of the gold precursor ($HAuCl_4$) solution can influence the formation rate, dispersion and size of AuNPs on ESM. At pH $\leq$3.0 and $\geq$7.0, no AuNPs are observed on ESM while small AuNPs are homogeneously dispersed on ESM at pH 4.0–6.0. The optimal pH for AuNPs formation on ESM is 6.0. AuNPs/ESMs are used to immobilize glucose oxidase (GO_x) for glucose biosensing. AuNPs on ESM can increase the enzyme activity of GO_x. The linear response range of the glucose biosensor is 20 μM to 0.80 mM glucose with a detection limit of 17 μM (S/N = 3). The biosensor has been successfully applied to determine the glucose content in commercial glucose injections. Our work provides a very simple, non-toxic, convenient, and green route to synthesize AuNPs on ESM which is potentially useful in the biosensing field.

1. Introduction

Metal nanoparticles (NPs) have attracted considerable attention for their unusual chemical and physical properties such that they show great potential applications in biotechnology, catalysis, medical imaging, novel electronics and optics [1–6]. Many methods have been developed for synthesizing metal NPs, especially gold nanoparticles (AuNPs) [7–12]. Recently there is an ever-growing need to develop clean, non-toxic and environmentally friendly ("green chemistry") synthetic procedures and researchers have been looking at biological systems for inspiration [13–15]. Consequently, a novel biological method for the synthesis of AuNPs and silver nanoparticles (AgNPs) using the fungus *Verticillium* was reported by Mukherjee et al. [16]. AuNPs and AgNPs of good monodispersity were formed as a result of the intracellular reduction of the metal ions when the fungal biomass was exposed to an aqueous solution of $AuCl_4^-$ or Ag^+ ions. Recently, Raveendran et al. [17] used a reducing sugar, β-D-glucose, as the reducing agent and starch as the capping agent, to prepare "green" starched AgNPs. Sucrose [18] and chitosan were also reported for the synthesis of AuNPs [19].

Biological systems form sophisticated mesoscopic and macroscopic structures within which the placement of nanoscopic building blocks can be manipulated or modified to extended architectures. There is quite a list of biological species and/or biomaterials including bacteria, cells, cellulose, DNA, enzymes, plant leaves and wool that have been used as templates for the formation of micrometer- and nanometer-sized inorganic structures [20–25]. However, it is still vital to explore other cheap, non-toxic and readily available biomaterials for synthesizing and incorporating NPs

* Corresponding author at: College of Chemical Engineering, Sichuan University, Chengdu 610064, PR China. Tel.: +86 28 85415029; fax: +86 28 85416029.
** Corresponding author. Tel.: +852 34117839; fax: +852 34117348.
E-mail addresses: xiaodan@scu.edu.cn (D. Xiao), mfchoi@hkbu.edu.hk (M.M.F. Choi).
[1] Exchange student on visit to Hong Kong Baptist University.
[2] Visiting scholar to Hong Kong Baptist University.

0039-9140/$ – see front matter © 2010 Elsevier B.V. All rights reserved.
doi:10.1016/j.talanta.2010.04.014

for analytical applications. To our knowledge, there is no report on the use of natural eggshell membrane (ESM) to synthesize AuNPs and then immobilize with enzyme for biosensing applications.

Hen egg is the most popular food in the world. ESM is the innermost portion of eggshell which comprises inner and outer layers and eggshells can be readily obtainable as waste from kitchens and industry [26]. ESM mainly contains proteins such as collagen (types I, V, and X), osteopontin and sialoprotein, and a small amount of saccharides [27]. A few applications of ESM including matrices for adsorption of heavy metal ions and dyes [28–30], biological dressings for burns [31], substrates for cell culture [32], platforms for enzyme immobilization [33–35] and PbS nanoclusters synthesis [36], and templates for forming ordered tube networks have been reported [37]. Herein, we present a facile and totally green method to in situ synthesize AuNPs on ESM (AuNPs/ESM) using only a buffered Au(III) complex ($HAuCl_4$) aqueous solution at ambient conditions. No external or added reducing agent is required to reduce Au(III) ions to AuNPs. Au(III) ions are initially adsorbed, in situ reduced by moieties of the ESM fibers to form Au^0 atoms which finally deposit on the ESM as AuNPs. In this article, the formation mechanisms of AuNPs on ESM are proposed. The effect of pH on the core size and distribution of AuNPs on ESM has been studied in detail. These AuNPs/ESMs were fully characterized by scanning electron microscopy (SEM), X-ray photoelectron spectroscopy (XPS), energy dispersive X-ray spectroscopy (EDS), and powder X-ray diffraction (XRD). As compared to other biosyntheses of AuNPs, our proposed method is simple, non-toxic, efficient and environmentally friendly. Furthermore, it is well known that AuNPs are very good electron conductors and can facilitate electron transfer in biosensors more efficiently [38,39]. Thus, AuNPs/ESMs were used to immobilize glucose oxidase (GO_x) to form GO_x-AuNPs/ESMs and the response of which to glucose was significantly enhanced. It is anticipated that our AuNPs/ESM can be readily adapted to devices to widen their applications in the fields of electrochemistry, chemo/biosensor and biocatalysis.

2. Experimental

2.1. Chemicals

β-D-Glucose and hydrogen tetrachloroaurate(III) trihydrate ($HAuCl_4{\cdot}3H_2O$) was obtained from Aldrich (Milwaukee, WI, USA). Sodium dihydrogen phosphate dihydrate and disodium hydrogen orthophosphate dihydrate were from Fluka (Buchs, Switzerland). Glucose oxidase (from *Aspergillus niger* with a specific activity of 235 U/mg of solid) and horseradish peroxidase (HRP with a specific activity of 51 U/mg of solid) were from Sigma (St. Louis, MO, USA). 4-Aminoantipyrine (AAP) and phenol were from Kelong (Chengdu, China). The buffer solutions used in this study were 50 mM phosphate at various pHs. Fresh eggs were bought from a local supermarket in Hong Kong. The water used in all the experiments was doubly distilled deionized (DDW).

2.2. Biosynthesis of AuNPs on ESM

An ESM was carefully peeled off from a broken fresh eggshell after the albumen and yolk had been removed. It was then cleansed with copious amounts of DDW to completely remove the albumen. The synthesis of AuNPs on natural ESM was performed as follow. The clean ESM was dried in air at ambient conditions and cut into small rectangular pieces (*ca* 5 × 8 mm). The weight of the pieces was controlled at 2.4 ± 0.1 mg for all experiments. The ESM was initially conditioned in a 50 mM phosphate buffer solution with a specified pH for 10 min. It was then immersed in a 1.0 mL buffered phosphate $HAuCl_4$ solution for 1.5 h. The pH of this buffer solution was the same as the previous condition phosphate buffer. The reaction was initiated by adsorption of the negatively charged Au(III) ions onto the surface of ESM. Au(III) ions were spontaneously reduced to Au atoms and deposited as AuNPs on the ESM. The yellow $HAuCl_4$ solution was slowly decolorized and the white ESM finally turned to light brown. The AuNPs-immobilized ESM was removed from the $HAuCl_4$ solution and rinsed with copious amounts of DDW to remove excess Au(III) ions. The AuNPs/ESM sample was air-dried at ambient conditions before further characterization.

2.3. Characterization of AuNPs/ESM

SEM images of AuNPs/ESM were captured on a LEO 1530 field emission scanning electron microscope (FESEM) (LEO Elektronenmikroskopie GmbH, Oberkochen, Germany) at an accelerating voltage of 5 kV. Elemental determination was performed on an energy dispersive X-ray spectrometer attached to the FESEM. The adsorption of $AuCl_4^-$ on the surface of ESM was monitored by recording the absorbance change of the $HAuCl_4$ solution. UV–vis absorption of the $HAuCl_4$ solution containing the ESM was conducted on a Varian Cary 300 UV–vis absorption spectrophotometer (Palo Alto, CA, USA) at 10-mm path-length. XPS measurements were conducted on a SKL-12 X-ray photoelectron spectrometer (Shenyang, China) equipped with a VG CLAM 4 MCD electron energy analyzer using an Mg Kα source. The applied voltage and current were 10 kV and 15 mA, respectively. The peak curve fitting was accomplished by a Casa XPS software package. All the peaks were corrected with the C 1s peak (carbon from the ESM) at 286.4 eV as the reference. Powder XRD patterns of the AuNPs/ESM samples were recorded on a Rigaku Rotaflex RU-200B powder X-ray diffractometer (The Woodlands, TX, USA) with Cu Kα radiation and a Ni filter. XRD patterns were recorded from 25 to 90° (2θ) with a scanning step of 0.02°.

2.4. Immobilization of GO_x on AuNPs/ESM and assessment of response to glucose

GO_x was immobilized on ESM or AuNPs/ESM by a cross-linking method [40]. 10-mm diameters of ESMs with and without AuNPs were firstly prepared. These membranes were cleansed with copious amounts of deionized water and placed in a clean watch glass. 100 μL of 1.0% (w/w) GO_x solution at pH 7.0 was added. After about 1 h, 20 μL of 2.5% (w/w) glutaraldehyde solution was dropped onto the surface of the membrane and left to stand 30 min. The membrane was then immersed in and washed with a pH 7.0 phosphate buffer solution for 5 min. After washing, the GO_x-immobilized eggshell membranes (GO_x/ESM or GO_x-AuNPs/ESM) were stored in a pH 7.0 phosphate buffer solution at 4 °C until further use.

In our preliminary work, a colorimetric method based on Trinder's reaction [41] was employed to assess the response of GO_x/ESM or GO_x-AuNPs/ESM to a glucose solution. GO_x/ESM or GO_x-AuNPs/ESM was placed in a 10.0-mL of 0.60 mM glucose solution (pH 7.0). 40 μL of HRP solution (0.70 mg mL^{-1}) was added and followed by 1.0 mL of AAP (0.40 mM) and phenol (40 mM) solution. An UV–vis absorption spectrophotometer was then used to assess the enzyme activity at 505 nm after this reaction mixture had been incubated at 37 °C for 15 min [42]. Subsequently, the optimal GO_x-AuNPs/ESM was employed to determine the glucose content of various commercial glucose injections. Calibration curves were constructed using the colorimetric method and glucose standards of various concentrations. Finally, the samples were diluted by a pH 7.0 phosphate buffer solution and then analyzed by the GO_x-AuNPs/ESM based on the colorimetric method.

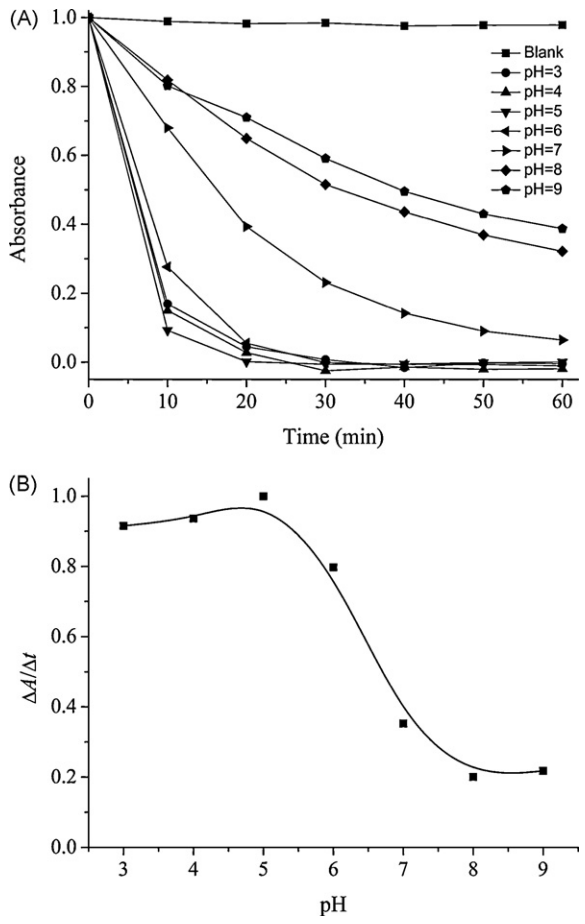

Fig. 1. (A) The absorbance changes at 250 nm of the buffered $HAuCl_4$ solutions containing eggshell membranes at various pHs (3.0–9.0). The initial concentration of $HAuCl_4$ was 0.25 mM. (B) The rate of change in absorbance at the first 10 min. Plot of $\Delta A/\Delta t$ against pH. A is the absorbance at 250 nm. ΔA is the difference of absorbance values at $t = 0$ and 10 min. The absorbance change and the rate of change in absorbance are normalized for ease of comparison.

3. Results and discussion

3.1. pH effect on adsorption of Au(III) ions on ESM

The pH of the solution is a very important factor to determine the adsorption of Au(III) ions on ESM. In order to investigate the effect of pH, the absorbance change of $HAuCl_4$ solution at 250 nm containing ESM at various pHs (3.0–9.0) was monitored and depicted in Fig. 1A. The absorbances were normalized at the beginning of the experiments for ease of comparison. It should be borne in mind that all Au(III) ions studied here show appreciable absorption at 250 nm (Fig. S1 of Supplementary Material). It is clearly observed that the absorbances decrease with the increase in reaction time, indicating that Au(III) ions are removed from the aqueous medium and adsorbed on ESM (*vide infra*). The change in absorbance of aqueous $HAuCl_4$ solution can indirectly indicate the adsorption rate of Au(III) ions on ESM. The adsorption rate is very fast at the first 10 min and then slows down with the increase in time. Fig. 1B shows the change of absorbance ($\Delta A/\Delta t$) as a function of pH at the first 10 min as in Fig. 1A. Again, $\Delta A/\Delta t$ is normalized for ease of comparison. The adsorption rate is higher at the acidic region (pH 3.0–6.0), indicating that slight acidic conditions favor the adsorption of Au(III) ions on ESM. The absorbance of the $HAuCl_4$ solution decreased by 95.5, 97.2, 99.8 and 94.5% at pH 3.0, 4.0, 5.0 and 6.0, respectively in the first 20 min. At pH 3.0–5.0, the adsorption rate increases with the increase in pH. However, when the pH increases to 6.0, the rate drops. On the other hand, at the neutral and slightly alkaline conditions (pH 7.0–9.0), the adsorption rate of Au(III) ions is much slower and decreases with the increase in pH at this range. The absorbance of the solution decreased by 71.0, 35.0 and 29.0% at pH 7.0, 8.0 and 9.0, respectively over the initial 20 min.

The decrease in absorbance of $AuCl_4^-$ aqueous solution in contact with ESM can be attributed to two main reasons: First, the surface charge of the ESM changes with pH. ESM comprises protein fibers which possess lots of amino and carboxylic moieties. The ESM protein fiber is also derived mainly from amino acids such as glycine and alanine. The isoelectric points of these two amino acids are 5.97 and 6.02, respectively [43]. At low pH (3.0–6.0), the amino moiety is protonated to form functional groups such as $-NH_3^+$ and $-N^+H_2-$. As such, the negatively charged $[AuCl_x(OH)_{4-x}]^-$ ions ($x \geq 2$) are electrostatically attached to the surface of ESM. By contrast, when the pH increases to 7.0–9.0, the surface charge of ESM are less positive with a concomitant decrease in the deposition of the $[AuCl_x(OH)_{4-x}]^-$ ions ($x < 2$). As a result, the change in absorbance of an $AuCl_4^-$ aqueous solution at high pH is much smaller and slower than at low pH.

In addition, when we compare the rate of decrease in absorbance at pH 3.0–5.0, it follows the trend: pH 5.0 > 4.0 > 3.0. The plausible reason is that the $[AuCl_x(OH)_{4-x}]^-$ ions ($x \geq 2$) consist of more OH^- when the pH increases in this range. It is well known that the size of OH^- is smaller than Cl^-. As such, the charge density for $[AuCl_x(OH)_{4-x}]^-$ ion will be higher if it contains more OH^-. Consequently, the electrostatic attraction will be stronger between the $[AuCl_x(OH)_{4-x}]^-$ ions and the protein fiber so that the decrease in absorbance is fastest at pH 5.0, followed by pH 4.0 and then pH 3.0.

3.2. Formation of AuNPs on ESM

As mentioned above, Au(III) ions can be easily adsorbed on ESM and the ESM turns slowly from white to pale yellow and then finally to light brown when it is in contact with an $AuCl_4^-$ solution. It is very probable that the surface-adsorbed Au(III) ions react with some reductant moieties of the ESM protein fibers to form AuNPs and the presence of AuNPs on the ESM can be verified by SEM, XPS and XRD analyses (*vide infra*). In fact, the pH of $HAuCl_4$ aqueous solution also influences the nucleation and growth of Au crystals on the substrate. Recently AuNPs with different sizes were synthesized by the reduction of $AuCl_4^-$ ions in aqueous or on the substrate by different kinds of reducing agents at various pH [44]. As such, the effect of pH on the growth of AuNPs on ESM was also explored in this work.

ESM comprises an intricate lattice meshwork of fibers at the inner surface of the eggshell [45]. The microstructure of ESM can be easily studied by SEM. Fig. 2 displays the SEM images of the ESMs before and after immersion in various buffered 0.76 mM $HAuCl_4$ solutions for 1.5 h. A network-like structure is observed on the natural ESM (Fig. 2A), indicating that ESM contains cavities and highly cross-linked protein fibers with diameters of 0.5–1.5 μm and pore sizes of *ca* 5 μm. It has been reported that collagen and saccharides are the main constituents of ESM. Collagen is a major protein in animal tissue and is the most abundant in vertebrates [46]. Nakano et al. [47] have also pointed out that the main chemical composition of chicken ESM are amino acids (glycine and alanine) and uronic acid. Thereby, lots of amino, hydroxyl and carbonyl functional groups on the ESM fibers are available to interact with the $[AuCl_x(OH)_{4-x}]^-$ ($x = 0$–4) ions. Among the main ingredients of ESM, only uronic acid and saccharides can possibly act as reductants to reduce the surface-adsorbed Au(III) ions to form AuNPs. Uronic acid is a product of sugar in which the terminal carbon's hydroxyl group has been oxidized to a carboxylic acid and so it contains both carboxylic acid and aldehyde moieties. The chemical structure of uronic acid is displayed in Fig. S2. Compounds containing alde-

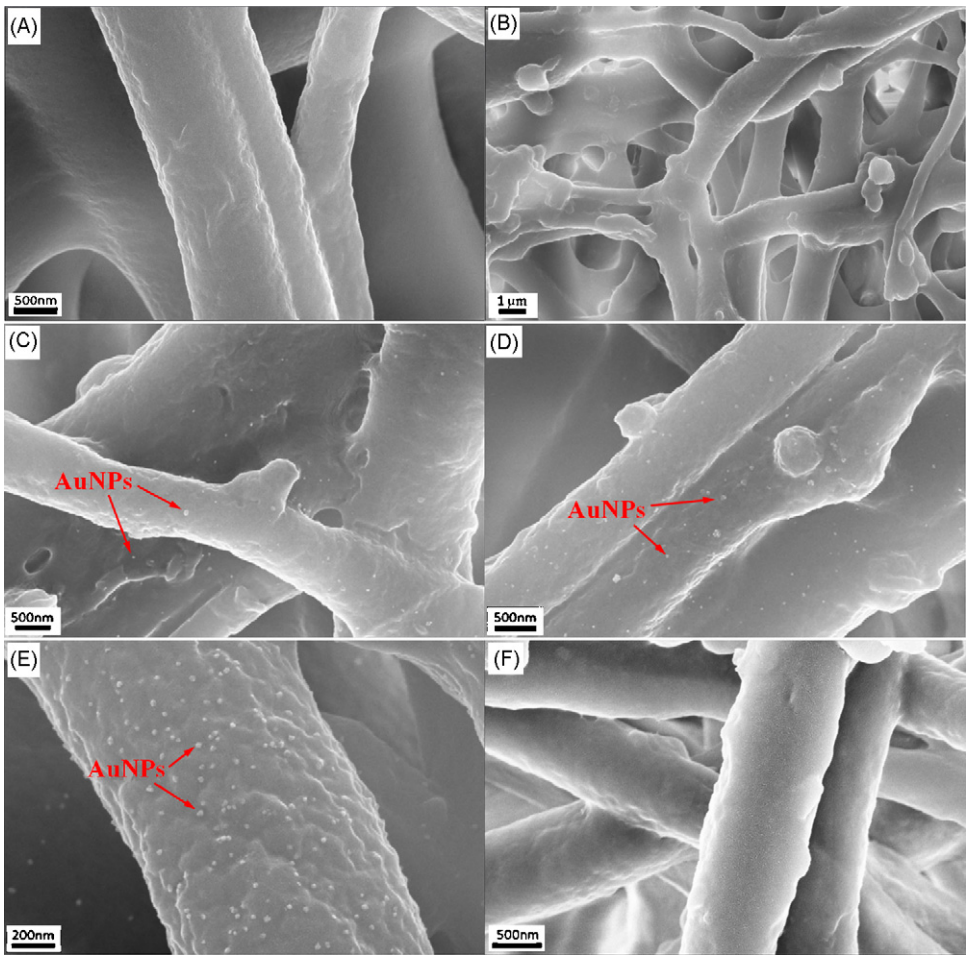

Fig. 2. Scanning electron micrographs of eggshell membranes after they had contacted with 0.76 mM $HAuCl_4$ solutions for 1.5 h under various pHs: (A) a natural eggshell membrane for comparison, (B) 3.0, (C) 4.0, (D) 5.0, (E) 6.0, and (F) 7.0.

hyde moieties are capable to reduce Au(III) to Au^0. This has been demonstrated by mixing cinnamaldehyde, *m*-nitro-benzaldehyde or β-D-glucose with $HAuCl_4$ solutions at which typical surface plasmon resonance bands were observed in their UV–vis absorption spectra (Fig. S3). Our results prove the facile formation of AuNPs from $HAuCl_4$ solution containing compounds with aldehyde moieties [48]. By contrast, glycine and alanine (Fig. S3) did not produce the same results [49]. As such, we can conclude that the aldehyde moiety of uronic acid and saccharides in ESM play a significant role in reducing the surface-adsorbed Au(III) ions to AuNPs.

SEM has been an essential tool for characterizing the surface morphology and fundamental physical properties of samples, and also for determining the particle shape and size distribution of AuNPs on solid substrates. The formation of AuNPs on the surface of ESM was evident via SEM studies. Fig. 2 visualizes the AuNPs deposited on the surface of the ESM fibers at various pHs. These AuNPs-immobilized ESMs were prepared by exposing the ESMs with 0.76 mM $HAuCl_4$ solutions at various pHs (3.0–6.0) for 1.5 h. The Au(III) ions were initially adsorbed on the ESM fibers under acidic conditions and followed with subsequent reduction by the R–CHO moieties (from uronic acid and saccharides of the ESM fibers) to AuNPs (see Eq. (1) of Supplementary Material).

It is interesting to note that not much AuNPs were formed on the ESM at pH 3.0 (Fig. 2B) although appreciable adsorption of Au(III) ions on ESM was observed at this pH (Fig. 1). It is plausible that this too acidic condition does not favor the reduction reaction. As indicated in Fig. 2C–E, the quantity of AuNPs on the surface of ESM increases with the increase in pH from 4.0 to 6.0, inferring that increasing pH is more favorable for the reduction reaction. However, when the pH increases to 7.0, it is difficult to observe any AuNPs on ESM (Fig. 2F) even though some adsorptions of Au(III) ions onto ESM are proved to have taken place (Fig. 1). Similarly, when the $HAuCl_4$ solution was at pH 8.0–9.0, it was hard to identify any AuNPs on ESM. Their SEM images (not shown here) looked exactly the same as a natural ESM. In essence, an optimal pH is needed to allow both adsorption and reduction of Au(III) ions on ESM to occur so that a noticeable amount of AuNPs can be efficiently formed. It is obvious that well-dispersed and uniform spherical AuNPs (25 ± 7 nm) can successfully grow on the surface of protein fibers at pH 6.0 (Fig. 2E). The SEM images show that the dispersion and deposition of AuNPs occurs without significant disruption to or modification of the fibrillar network of ESM. As such, pH 6.0 was chosen for most of our studies (*vide infra*).

The formation of AuNPs on the surface of ESM can also be confirmed by EDS as depicted in Fig. 3A. A spot-profile energy dispersive analysis of X-ray of one of the AuNPs clearly shows the characteristics Au^0 peaks at 2.12 and 9.78 keV [50] whereas other peaks were C, N and O of the ESM. Other spots of AuNPs on ESM display similar EDS. Our EDS analysis corroborates the presence of AuNPs and the absence of Cl^-, inferring the complete reduction of Au^{3+} to Au^0. In addition, the crystalline structure of AuNPs on ESM was characterized by the powder XRD technique. The ESM sample had to be exposed to a more concentrated solution of $HAuCl_4$ (2.54 mM) for 1.5 h in order to acquire better and stronger diffraction peak signals. Fig. 3B shows the XRD patterns of ESM before and after immobilization of AuNPs. Natural ESM is almost amor-

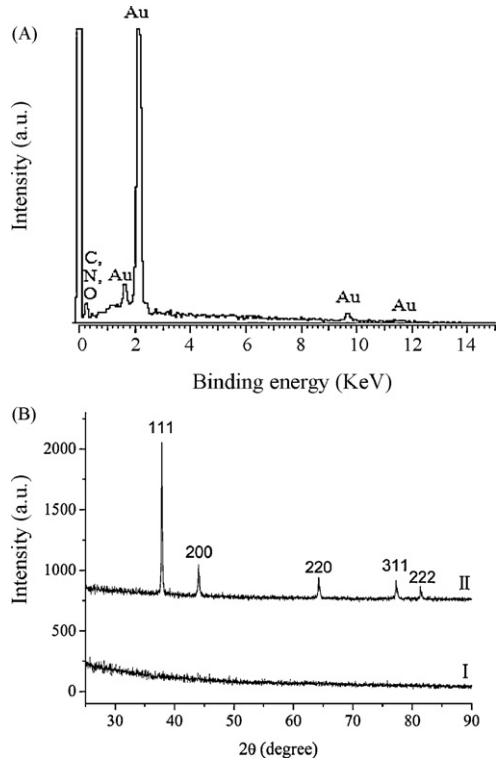

Fig. 3. (A) Spot-profile EDS spectrum recorded from one of the gold nanoparticles on eggshell membrane. (B) XRD patterns of (I) natural eggshell membrane and (II) gold nanoparticles-immobilized eggshell membrane. The eggshell membranes used for EDX and XRD were all prepared from immersing the membranes in 2.54 mM $HAuCl_4$ solutions at pH 6.0 for 1.5 h.

phous without any diffraction peak (Fig. 3B(I)) as its ingredients are mainly amines, amides, and carboxylic compounds. By contrast, clear diffraction peaks are observed for the AuNPs/ESM as depicted in Fig. 3B(II). These peaks are assigned to diffraction from the {1 1 1}, {2 0 0}, {2 2 0}, {3 1 1}, and {2 2 2} planes of face center cubic (fcc) Au crystal which are in complete agreement with the Joint Committee on Powder Diffraction Standards (JCPDS card no. 04-0784). Again, the XRD data confirm the formation of typical fcc structure of polycrystalline AuNPs on ESM. Moreover, the oxidation state of Au species in AuNPs was studied by XPS and is displayed in Fig. S4. C 1s, N 1s, O 1s, and Au 4f peaks were identified in the spectrum. The Au $4f_{5/2}$ and Au $4f_{7/2}$ peaks with the binding energies of 84.0 and 87.7 eV were clearly observed (Fig. S4B), respectively which are typical binding energies for Au atoms [51]. The XPS results are in consistent with XRD and EDS data that zerovalent gold atoms are formed on ESM.

3.3. Response of GO_x-AuNPs/ESM to glucose

Gold is not only one of the best conductor among metals but it also has good biocompatibility. AuNPs is one of the most important NPs used to fabricate biosensors. AuNPs can provide a biocompatible environment for survival of enzyme [38] and therefore facilitate efficient electron transfer in biosensors. Recently, reports on enzymes connected to AuNPs for bioelectrocatalytic analysis show that the presence of AuNPs can improve the rate of electron transfer and thus increase the sensitivity of enzymes to substrates [38,39]. To further explore the potential use of our AuNPs/ESM for biosensing, various AuNPs/ESMs immobilized with GO_x were prepared and tested with a glucose solution. Seven samples of AuNPs/ESMs prepared with different concentrations of $HAuCl_4$ solution: (a) 0.00, (b) 0.25, (c) 0.76, (d) 1.27, (e) 1.78, (f) 2.54, and (g) 5.08 mM were initially fabricated. Each ESM sample of the same weight and size was preconditioned in a pH 6.0 phosphate buffer for 10 min before coating with AuNPs. Fig. 4 shows that the AuNPs/ESM samples get gradually darker, from white to light brown and then deep brown with the increase in concentration of $HAuCl_4$, indicating the increase of AuNPs coated on ESM. The color of these AuNPs/ESMs did not change after several months of storage at ambient conditions. These ESM and AuNPs/ESM samples were subsequently immobilized with the same amount of GO_x by using a glutaraldehyde cross-linking method. Afterwards, each GO_x-ESM or GO_x-AuNPs/ESM sample was exposed to a 0.60 mM glucose solution (pH 7.0) and followed by the addition of HRP, AAP and phenol. The response of GO_x-AuNPs/ESM to glucose can be assessed by monitoring the absorbance of red quinoneimine dye at 505 nm [42]. The typical reaction scheme is displayed as Eqs. (2) and (3) (Supplementary Material). The absorbance of the solutions at 505 nm containing GO_x-ESM and GO_x-AuNPs/ESM samples is shown in Fig. S5. The absorbance of the solution infers the sensitivity of a GO_x-AuNPs/ESM to glucose. GO_x-AuNPs/ESM samples produced higher absorbances than GO_x-ESM, indicating that AuNPs can enhance the sensitivity of glucose detection. This may be attributed to the increase of electron transfer rate in the catalytic oxidation of glucose to gluconic acid by AuNPs. However, when AuNPs on ESM is excessive, the sensitivity to glucose detection drops as depicted in Figs S5E and F. It is possible that too many and/or too large AuNPs deposited on the ESM will hinder the adsorption and cross-linking of GO_x onto the ESM fibers, resulting in lower sensitivity of glucose detection. Our results demonstrate that 0.76 mM $HAuCl_4$ solution (pH 6.0) is the optimum solution for preparing AuNPs/ESM which can produce the best sensitivity

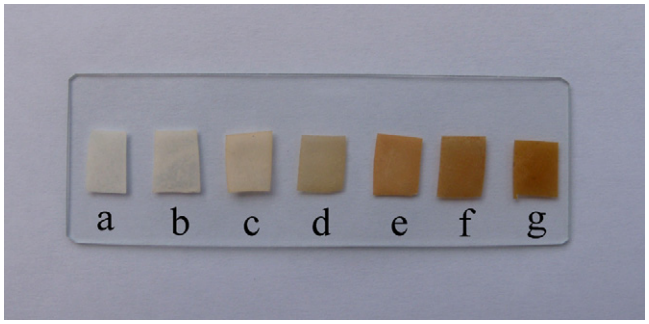

Fig. 4. Optical images of gold nanoparticles-immobilized eggshell membranes prepared from various concentrations of $HAuCl_4$ solutions at pH 6.0 for 1.5 h: (a) 0.00, (b) 0.25, (c) 0.76, (d) 1.27, (e) 1.78, (f) 2.54, and (g) 5.08 mM.

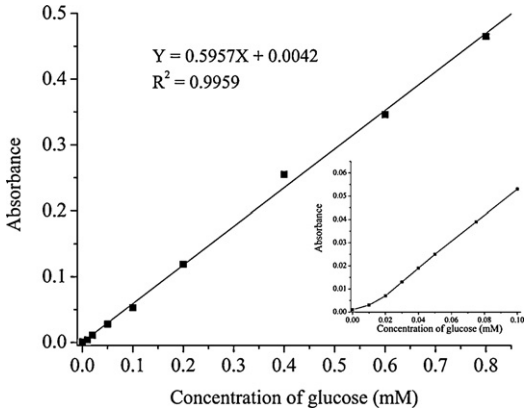

Fig. 5. Typical calibration curve of the GO_x-AuNPs/ESM glucose biosensor. The inset displays the response of biosensor to the lower glucose concentration range.

Table 1
Comparison of analytical performance of various nanoparticles-based glucose biosensors.

Analytical performance	Nanoparticles-based glucose biosensors				
	AuNPs/ESM (this work)	Chitosan-Fe_3O_4 [52]	Pt-SiO_2 [53]	Pt [54]	Pd [55]
Linear range	20 μM to 0.80 mM	500 μM to 22 mM	30 μM to 3.8 mM	250 μM to 2.0 mM	500 μM to 30 mM
Detection limit (S/N = 3)	17 μM	500 μM	20 μM	150 μM	75 μM
Shelf-life	87.3% After 70 days	80% After 8 weeks	90%After 23 days	1 month	75% After 12 days

Table 2
Determination and recovery of glucose in glucose injections using the GO_x-AuNPs/ESM glucose biosensor.

Sample[a]	Claimed glucose concentration (g/100 mL)	Concentration of glucose[b] (g/100 mL)	RSD[c] (%)	Glucose added (mM)	Glucose found (mM)	Recovery (%)	RSD[c] (%)
1	5	4.63	8.03	0.250	0.235	94.0	3.03
2	10	10.1	6.56	0.250	0.253	101	5.19
3	50	50.9	4.94	0.250	0.251	100	4.23
4	50	50.7	1.61	0.250	0.248	99.2	1.97
5	50	52.4	3.73	0.250	0.236	94.4	8.80

[a] Samples of glucose injection were obtained from different companies.
[b] Determined by this work.
[c] Three replicates were performed.

of glucose detection. As such, this GO_x-AuNPs/ESM was chosen for real sample analysis.

3.4. Analytical performance of the glucose biosensor and sample analysis

The optimal GO_x-AuNPs/ESM was employed to construct a glucose biosensor based on the colorimetric method (*vide supra*). The response of this GO_x-AuNPs/ESM glucose biosensor to various concentrations of glucose was conducted in a pH 7.0 phosphate solution at 37 °C. Fig. 5 shows a typical response curve of the proposed glucose biosensor. The absorbance of the solution increases with the increase in glucose concentration. A linear calibration curve between the glucose concentration and the absorbance of the solution was obtained. The inset of Fig. 5 displays the response to lower glucose concentration. The plot reveals that the biosensor has a good linear response to glucose ranging 20 μM to 0.80 mM and the detection limit was 17 μM (S/N = 3).

The operation stability of the biosensor was evaluated by repetitive measurements (n = 5) of its response to 0.25 mM glucose. The response did not change much during this period with a R.S.D. of 2.98%. The biosensor retained 87.3% of its initial response after 70 days of storage at 4 °C and thus demonstrates a long shelf-life. Table 1 compares the analytical performances of various nanoparticles-based glucose biosensors [52–55] with that of our proposed biosensor. It can be seen that our biosensor performs better.

To illustrate the feasibility of the glucose biosensor in practical analysis, it was employed to measure the glucose content in some commercial glucose injections. The glucose injections were diluted by a pH 7.0 phosphate buffer to yield testing sample solutions. In addition, the recovery test was conducted. The data are summarized in Table 2. The results demonstrate that our proposed glucose biosensor offers an excellent and accurate method for glucose determination. Potential interfering substrates were evaluated to assess the selectivity of the glucose biosensor. The results show that 100-fold of Na^+, Mg^{2+}, K^+, NO_3^-, HCO_3^-, SO_4^{2-}, and Cl^- did not cause any interference on the response of the biosensor.

4. Conclusion

In summary, we have successfully developed an effective, simple and green synthetic route for AuNPs via a biomaterial. Natural ESM can serve as reactive substrate and some of the active functional groups of ESM fibers can act as reductants for the Au(III) ions. The formation of AuNPs on ESM is mainly driven by adsorption of Au(III) ions on the ESM fiber, reduction by aldehyde moiety of the fiber, and nucleation of NPs. The synthesis of AuNPs on the surface of ESM is influenced by pH as pH affects the adsorption and reduction of Au(III) ions on ESM. The adsorption rate is quicker at low pH (3.0–6.0) than at high pH (7.0–9.0) whereas the reduction is more favorable at slightly alkaline conditions. The optimal pH is determined to be 6.0 at which more and smaller AuNP crystals are produced. The major attributes of our work are that no external reductant is required, non-toxic biomaterial is used, and the synthetic route is simple at ambient conditions. Finally, it is worth to say that Au nanocrystals are aesthetically pleasing, chemically noble, and environmentally benign [12]. GO_x-AuNPs/ESM can improve the sensitivity of glucose detection when compared with GO_x-ESM. It has been applied to determine the glucose content in some commercial products. Our biocompatible nanocomposites AuNPs/ESM are very promising for applications in a wide range in the biosensor and biocatalysis fields. Our laboratories are currently exploring other analytical applications of these AuNPs/ESMs.

Acknowledgements

We would express our sincere thanks to Mr. Tommy W.H. Poon of the Department of Chemistry, Hong Kong Baptist University for acquiring the SEM images and EDS, and Ms. Y.K. Wu of the Centre for Surface Analysis and Research, Hong Kong Baptist University for the XPS and XRD measurements. Financial support from the Research Grants Council of the Hong Kong Special Administrative Region, China (project no. HKBU 200907) is gratefully acknowledged.

Appendix A. Supplementary data

Supplementary data associated with this article can be found, in the online version, at doi:10.1016/j.talanta.2010.04.014.

References

[1] G. Schmid, Chem. Rev. 92 (1992) 1709.
[2] Y. Voloktitin, J. Sinzig, L.J. Jong, G. Schmid, M.N. Vargaftik, I.I. Moiseev, Nature 384 (1996) 621.
[3] A.N. Shipway, E. Katz, I. Willner, Chem. Phys. Chem. 1 (2000) 18.
[4] Y. Cao, R. Jin, C.A. Mirkin, J. Am. Chem. Soc. 123 (2001) 7961.
[5] Y. Xia, N.J. Halas, MRS Bull. 30 (2005) 338.
[6] Y. Lee, A. Loew, S. Sun, Chem. Mater., doi:10.1021/cm9013046.

[7] M. Brust, M. Walker, D. Bethell, D.J. Schiffrin, R.J. Whyman, J. Chem. Soc., Chem. Commun. (1994) 801.
[8] M.J. Hosteler, J.E. Wingate, C.J. Zhong, J.E. Harris, R.W. Vachet, M.R. Clark, J.D. Londono, S.J. Green, J.J. Stokes, G.D. Wignall, G.L. Glish, M.D. Porter, N.D. Evans, R.W. Murray, Langmuir 14 (1998) 17.
[9] Y. Sun, Y. Xia, Science 298 (2002) 2176.
[10] K.S. Mayya, B. Schoeler, F. Caruso, Adv. Funct. Mater. 13 (2003) 183.
[11] M.K. Corbierre, R.B. Lennox, Chem. Mater. 17 (2005) 5691.
[12] R. Sardar, A.M. Funston, P. Mulvaney, R.W. Murray, Langmuir 25 (2009) 13840.
[13] A. Lapkin, L. Joyce, B. Crittenden, Environ. Sci. Technol. 38 (2004) 5815.
[14] C. Engelbrekt, K.H. Sørensen, J.D. Zhang, A.C. Welinder, P.S. Jensen, J. Ulstrup, J. Mater. Chem. 19 (2009) 7839.
[15] M.N. Nadagouda, G. Hoag, J. Collins, R.S. Varma, Cryst. Growth Des. 9 (2009) 4979.
[16] P. Mukherjee, A. Ahmad, D. Mandal, S. Senapati, S.R. Sainkar, M.I. Khan, R. Ramani, R. Parischa, P.V. Ajayakumar, M. Alam, M. Sastry, R. Kumar, Angew. Chem. Int. Ed. 40 (2001) 3585.
[17] P. Raveendran, J. Fu, S.L. Wallen, J. Am. Chem. Soc. 125 (2003) 13940.
[18] Z. Qi, H. Zhou, N. Matsuda, I. Honma, K. Shimada, A. Takatsu, K. Kato, J. Phys. Chem. B 108 (2004) 7006.
[19] H. Huang, X. Yang, Biomacromolecules 5 (2004) 2340.
[20] J.H. He, T. Kunitake, A. Nakao, Chem. Mater. 15 (2003) 4401.
[21] Z. Li, S.W. Chung, J.M. Nam, D.S. Ginger, C.A. Mirkin, Angew. Chem. Int. Ed. 42 (2003) 2306.
[22] G. Wei, H.L. Zhou, Z.G. Liu, Y.H. Song, L. Wang, L.L. Sun, Z. Li, J. Phys. Chem. B 109 (2005) 8738.
[23] I. Willner, R. Baron, B. Willner, Adv. Mater. 18 (2006) 1109.
[24] E. Kharlampieva, J.M. Slocik, T. Tsukruk, R.R. Naik, V.V. Tsukruk, Chem. Mater. 20 (2008) 5822.
[25] S.K. Nune, N. Chanda, R. Shukla, K. Katti, R.R. Kulkarni, S. Thilakavathy, S. Mekapothula, R. Kannan, K.V. Katti, J. Mater. Chem. 19 (2009) 2912.
[26] D.A. Carrino, J.E. Dennis, T.M. Wu, J.L. Arias, M.S. Fernandez, J.P. Rodriguez, D.J. Fink, A.H. Heuer, A.I. Caplan, Connect. Tissue Res. 35 (1996) 325.
[27] Y. Nys, J. Gautron, M.D. McKee, J.M. Gautron, M.T. Hincke, World Poultry Sci. J. 57 (2001) 401.
[28] B. Koumanova, P. Peeva, S.J. Allen, K.A. Gallagher, M.G. Healy, J. Chem. Tech. Biotech. 77 (2002) 539.
[29] M. Arami, N.Y. Limaee, N.M. Mahmoodi, Chemosphere 65 (2006) 1999.
[30] G. Annadurai, L.Y. Ling, J.F. Lee, J. Hazard. Mater. 152 (2008) 337.
[31] K. Maeda, Y. Sasaaki, Burns 8 (1984) 313–316.
[32] M. Tavassoli, Experientia 39 (1983) 411.
[33] M.M.F. Choi, W.S.H. Pang, D. Xiao, X.J. Wu, Analyst 126 (2001) 1558.
[34] B.L. Wu, G.M. Zhang, S.M. Shuang, M.M.F. Choi, Talanta 64 (2004) 546.
[35] Y. Zhang, G.M. Wen, Y.H. Zhou, S.M. Shuang, C. Dong, M.M.F. Choi, Biosens. Bioelectron. 22 (2007) 1791.
[36] H. Su, J. Han, N. Wang, Q. Dong, D. Zhang, C. Zhang, Smart Mater. Struct. 17 (2008) 015045.
[37] D. Yang, L.M. Qi, J.M. Ma, Adv. Mater. 14 (2002) 1543.
[38] Q. Xu, C. Mao, N.N. Liu, J.J. Zhu, J. Sheng, Biosens. Bioelectron. 22 (2006) 768.
[39] X.L. Ren, X.W. Meng, F.Q. Tang, Sens. Actuators B 110 (2005) 358.
[40] D. Xiao, M.M.F. Choi, Anal. Chem. 74 (2004) 863.
[41] J. Lott, K. Turner, Clin. Chem. 21 (1975) 1754.
[42] S. Rauf, A. Ihsan, K. Akhtar, M.A. Ghauri, M. Rahman, M.A. Anwar, A.M. Khalid, J. Biotechnol. 121 (2006) 351.
[43] V. Aristov, O.V. Bobreshova, S.Y. Eliseev, P.I. Kulintsov, Russ. J. Electrochem. 36 (2000) 323.
[44] V. Kozlovskaya, E. Kharlampieva, S. Chang, R. Muhlbauer, V.V. Tsukruk, Chem. Mater. 21 (2009) 2158.
[45] M. Wong, J.C. Hendrix, K. von der Mark, C. Little, R. Stern, Dev. Biol. 104 (1984) 28.
[46] S.J. Allen, M. McCallen, M.G. Healy, M. Wolki, P. Ulbig, Adsorption Science and Technology, World Scientific, Singapore, 2000, 46–50.
[47] T. Nakano, N.I. Ikawa, L. Ozimek, Poultry Sci. 82 (2003) 510.
[48] J.A. Creighton, G.D. Eadon, J. Chem. Soc. Faraday Trans. 87 (1991) 3881.
[49] Y.F. Li, X.W. Shen, C.Z. Huang, J. Wang, Chinese J. Anal. Chem. 6 (2008) 819.
[50] S.K. Das, A.R. Das, A.K. Guha, Langmuir 25 (2009) 8192.
[51] Y.C. Liu, T.C. Chuang, J. Phys. Chem. B 107 (2003) 12383.
[52] A. Kaushik, R. Khan, P.R. Solanki, P. Pandey, J. Alam, S. Ahmad, B.D. Malhotra, Biosens. Bioelectron. 24 (2008) 676.
[53] X.L. Ren, X.W. Meng, F.Q. Tang, L. Zhang, Mater. Sci. Eng. C 29 (2009) 2234.
[54] K. Yao, Y.H. Zhu, X.L. Yang, C.Z. Li, Mater. Sci. Eng. C 28 (2008) 1236.
[55] P. Santhosh, K.M. Manesh, S. Uthayakumar, S. Komathi, A.I. Gopalan, K.P. Lee, Bioelectrochemistry 75 (2009) 61.